



## Enhanced nitrate removal from groundwater using a conductive spacer in flow-electrode capacitive deionization

Hongjie Guo<sup>a,b</sup>, Qiang Wei<sup>b</sup>, Yangyang Wu<sup>b</sup>, Wei Qiu<sup>c</sup>, Hongliang Li<sup>a</sup>, Changyong Zhang<sup>b,\*</sup>

<sup>a</sup> College of Mining Engineering, Taiyuan University of Technology, Taiyuan 030024, China

<sup>b</sup> CAS Key Laboratory of Urban Pollutant Conversion, Department of Environmental Science and Engineering, University of Science and Technology of China, Hefei 230026, China

<sup>c</sup> CAS Key Laboratory of Mechanical Behavior and Design of Materials, Department of Modern Mechanics, University of Science and Technology of China, Hefei 230026, China

### ARTICLE INFO

#### Article history:

Received 17 August 2023  
Revised 16 November 2023  
Accepted 17 November 2023  
Available online 19 November 2023

#### Keywords:

Flow-electrode capacitive deionization  
Carbon cloth  
Nitrate  
Underground water  
Ions transport

### ABSTRACT

Flow-electrode capacitive deionization (FCDI) represents a promising approach for ion separation from aqueous solutions. However, the optimization of spacer, particularly for nitrate-contaminated groundwater systems, has often been overlooked. This research comprehensively investigates the influence of using a conductive (carbon cloth, CC) spacer on nitrate removal performance within FCDI system, comparing it to a non-conductive (nylon net, NN) spacer. In both CC and NN FCDI systems, it is unsurprisingly that nitrate removal efficiency improved notably with the increasing current density and hydraulic retention time (HRT). Interestingly, the specific energy consumption (SEC) for nitrate removal did not show obvious fluctuations when the current density and HRT varied in both systems. Under the auspiciously optimized process parameters, CC-FCDI attained a 20% superior nitrate removal efficiency relative to NN-FCDI, accompanied by a notably diminished SEC for CC-FCDI, registering at a mere 28% of NN-FCDI. This great improvement can be primarily attributed to the decrement in FCDI internal resistance after using conductive spacer, which further confirmed by electrochemical tests such as linear sweep voltammetry (LSV) and electrochemical impedance spectroscopy (EIS). Upon prolonged continuous nitrate removal at the optimized conditions, the CC-FCDI system achieved a consistent 90% nitrate removal efficiency with a low SEC of 2.7–7.8 kWh/kg NO<sub>3</sub>-N, underscoring its steady performance. Overall, this study highlights the pivotal importance of careful spacer design and optimization in realizing energy-efficient groundwater treatment via FCDI.

© 2024 Published by Elsevier B.V. on behalf of Chinese Chemical Society and Institute of Materia Medica, Chinese Academy of Medical Sciences.

Nitrate (NO<sub>3</sub><sup>-</sup>) contamination has emerged as a global water quality issue due to the escalation of agricultural practices [1–3]. Significant health concerns arise from its conversion to toxic nitrite within the human digestive system [4]. Numerous studies suggest a direct correlation between elevated nitrate levels in drinking water and the occurrence of methaemoglobinaemia (“blue baby syndrome”), a condition to which infants are particularly vulnerable [5]. Therefore, the increase in human-caused inputs has resulted in significant impacts on aquatic ecosystems, as well as posing potential health risks to both humans and livestock [6–8]. World Health Organization (WHO) has set maximum contaminant levels for NO<sub>3</sub><sup>-</sup> in drinking water at 50 mg/L (equivalent to 11 mg/L as NO<sub>3</sub>-N) [9]. Physico-chemical technologies including

ion-exchange [10,11], electrodialysis (ED) [12], and chemical reduction [13–17] were employed for NO<sub>3</sub><sup>-</sup> removal from source waters. Although these technologies have been reported to achieve high removal efficiencies, they demand relatively severe operating conditions (e.g., high chemical consumptions for ion-exchange [18] and high voltage for ED), thereby immensely increasing operational costs.

In the past two decades, great efforts have been devoted to capacitive deionization (CDI) [19–22]. Flow-electrode capacitive deionization (FCDI), a variant of CDI, has been recognized as an innovative and energy-efficient electrochemically driven ion separation technology [23,24]. Compared to conventional CDI that utilizes static electrodes, flowable electrodes are employed in FCDI systems, which can potentially achieve continuous running primarily due to the uninterrupted supply of new or regenerated particle electrodes into the flow-channels [25]. Previous studies have demonstrated that FCDI is effective for continuous removal

\* Corresponding author.

E-mail address: [changyongzhang@ustc.edu.cn](mailto:changyongzhang@ustc.edu.cn) (C. Zhang).

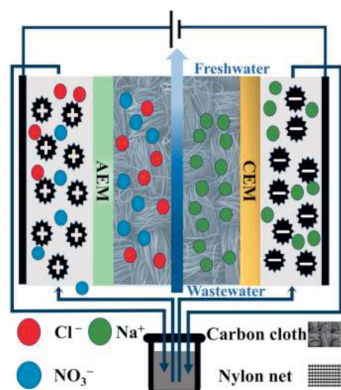


Fig. 1. The operation system of the CC-FCDI.

of  $\text{NO}_3\text{-N}$  with the effluent concentration below  $1\text{ mg/L}$  at a low energy consumption of  $\sim 0.5\text{ kWh/m}^3$  [26]. In an effort to further enhance the performance of FCDI, numerous studies have explored to optimize the FCDI architectures and develop innovative electrodes/membranes [23,27–29]. Note that the conductivity of flowable electrodes is 1–2 orders of magnitude lower than that of the fixed electrodes, much attention has been paid to elevate the conductivity of the flow electrodes (*e.g.*, increasing the content of the activated materials, and/or adding conductive additives) [30,31]. However, sporadic attention has been directed towards optimizing the spacer.

It should be noticed that spacer plays a significant role in FCDI devices [32], acting as support for the separators (*e.g.*, ion exchange membranes (IEMs) and creating feedwater flow channels, and promoting mixing [33]. Enhanced mixing can facilitate the minimization of concentration polarization, thereby reducing the non-ohmic resistance [34]. Unfortunately, these spacers have a notable drawback as they reduce the effective area of the IEMs for ionic conduction, leading to the elevation of internal resistance of FCDI unit, and thus dramatically increasing the energy consumption of the system especially when treating low-salinity feed streams [35,36]. Therefore, it is crucial to select or design suitable spacers to enhance the performance of FCDI. Another common strategy is the employment of conductive spacers. Tang and Zhou introduced ion-exchange resins as conductive spacer in desalination chamber, and found that interfacial electroconvection and charge efficiency was significantly enhanced [37]. Luo *et al.* improved the system by inserting a titanium mesh in the desalination chamber, which resulted in a 17.5% reduction in the specific energy consumption (SEC) [38]. They further enhanced the desalination performance of FCDI system by optimizing the architecture of the conductive spacer, achieving a 56.6% decrease in the SEC [39]. Previous studies have focused on the effect of titanium mesh-based conductive spacer additions on the desalination performance of FCDI. While these advances shed light on optimizing FCDI desalination performance, there remains a research gap concerning the impact of spacers on  $\text{NO}_3\text{-N}$  removal efficiency and SEC in groundwater system.

In this study, we incorporated carbon cloth (CC) into FCDI feed chamber as conductive spacer (Fig. 1), and compared the  $\text{NO}_3\text{-N}$  removal performances with the FCDI using traditional non-conductive nylon net (NN) spacer. The effects of current density and hydraulic retention time (HRT) on the performance of FCDI and SEC related to  $\text{NO}_3\text{-N}$  elimination were investigated. Electrochemical analysis such as linear sweep voltammetry (LSV) and electrochemical impedance spectroscopy (EIS) was conducted to further evaluate the critical role of CC played in FCDI system. Finally, the system was operated continuously for a duration of 9 h in order to investigate the robustness of CC in an FCDI unit.

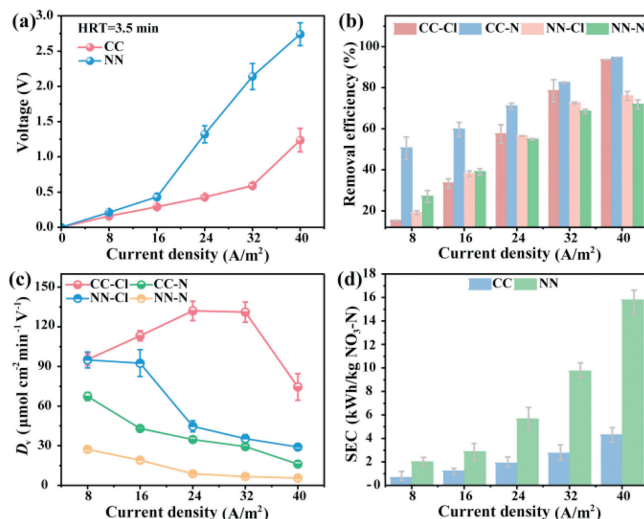


Fig. 2. Changes of the (a) cell voltages, (b)  $\text{NO}_3\text{-N}$  or  $\text{Cl}^-$  removal efficiency, (c)  $D_v$ , and (d) SEC as a function of the current density. The experiments were carried out in single-pass mode with the HRT set at 3.5 min. Each test was operated for a duration of 30 min.

All chemicals used in this study were obtained from Sigma-Aldrich with a purity level of greater than 99.0% (ACS grade), and were used without additional purification. Detailed information on material preparation, characterization, experimental analysis, and FCDI setup is presented in Text S1 and Fig. S1 (Supporting information).

Fig. 2a presents the variation cell voltage in relation to the applied current density. A breaking point in NN-FCDI was observed when the current density reached about approximately  $16\text{ A/m}^2$ . Beyond this point, the voltage increased more rapidly, reaching  $2.2\text{ V}$  at  $32\text{ A/m}^2$ . Even though the cell voltage of CC-FCDI also exhibited a similar increasing trend, the increase rate was half as much with a significantly higher breaking-point of  $32\text{ A/m}^2$ . Fig. 2b illustrates that a positive relationship was observed between the current density and the removal capacity of the FCDI. Compared to NN-FCDI, CC-FCDI maintained high  $\text{NO}_3^-$  removal efficiency (50%–60%) even at lower current densities ( $8\text{--}16\text{ A/m}^2$ ). Importantly, a notable  $\text{NO}_3\text{-N}/\text{Cl}^-$  selectivity up to 3.4 was observed when operating at a current density of  $8\text{ A/m}^2$ , indicating that  $\text{NO}_3^-$  is preferentially removed at low current densities compared to  $\text{Cl}^-$ . CC-FCDI achieved a  $\text{NO}_3\text{-N}$  removal rate of 82.4% at  $32\text{ A/m}^2$ , significantly higher than that of the NN-FCDI. More detailed information regarding this remarkable difference is further highlighted in Fig. S3 (Supporting information). This phenomenon may be attributed to the heightened affinity and passive adsorption tendencies exhibited by  $\text{NO}_3^-$  ions in comparison to  $\text{Cl}^-$  ions towards the anion exchange membrane (AEM) at low current density. Higher current densities tend to promote competitive migration of  $\text{NO}_3^-$  and  $\text{Cl}^-$  through the AEM, subsequently reducing  $\text{NO}_3\text{-N}/\text{Cl}^-$  selectivity (Fig. S4a in Supporting information). While the average salt removal rate (ASRR) of CC-FCDI and NN-FCDI systems are similar under the same current densities, cell voltages showed significant variations. As the current density increased, ASRR consistently rose and the corresponding voltage also increased. Once the threshold voltage was exceeded, there was a considerable drop in voltage-driven desalination capability ( $D_v$ ) that can be used to compare the rate of ion removal when the system is operated under different conditions. At a current density of  $32\text{ A/m}^2$ , the  $D_v$  of CC-FCDI was  $29.4\text{ }\mu\text{mol cm}^{-2}\text{ min}^{-1}\text{ V}^{-1}$  that was 3.4 time of the  $D_v$  of NN-FCDI (Fig. 2c). Correspondingly, higher current densities caused lower conductivity in the desalination chamber result-

ing in an increase in FCDI internal resistance, and thus higher energy costs (Fig. 2d). While our results indicate that CC-FCDI had the ability to reduce nitrate concentrations in contaminated groundwater to 1 mg NO<sub>3</sub>-N/L, achieving around 80% NO<sub>3</sub>-N removal efficiency (i.e., 10 mg NO<sub>3</sub>-N L<sup>-1</sup>) that conforms the World Health Organization (WHO) demand would be more cost-effective. On balance, it can be argued that 32 A/m<sup>2</sup> with an effluent concentration of less than 10 mg NO<sub>3</sub>-N/L and a SEC of 2.7 kWh/kg NO<sub>3</sub>-N is optimal for operation.

As shown in Fig. 3a, it was clear that the cell voltage of CC-FCDI is much lower than that of NN-FCDI. As HRT increased, both the voltages of CC-FCDI and NN-FCDI increased essentially linearly, but the CC-FCDI slope was smaller. The result was attributed to more moderate fluctuations in concentration level of the feed water in CC-FCDI [40]. The shear rate near the interface between the membrane and water decreased, resulting in an expansion of the diffusion boundary layer with the HRT increasing. The concentration at the membrane-water interface and the concentration of the influent water differed from one another more and more. Obviously, CC largely increased convection and reduced the expansion of the diffuse boundary layer. The distribution of feed water across the IEMs was observed to be more uniform, which reduced the non-ohmic resistance compared with NN-FCDI. Fig. 3b depicts the giant difference of CC-FCDI and NN-FCDI in removal efficiency. At the HRT of 3.5 min, the nitrate removal rate of CC-FCDI was about 15% higher than that of NN-FCDI. What can be noticed is that the change in HRT has little effect on the  $D_v$  of the system (Fig. 3c). It should be noted that the degree of NO<sub>3</sub><sup>-</sup> concentration reduction exhibited a linear relationship with the decrease of  $D_v$  (Fig. S5 in Supporting information). Specifically, the SEC increased from 2.2 kWh/kg NO<sub>3</sub>-N to 2.7 kWh/kg NO<sub>3</sub>-N across the HRT range of 2.5–3.5 min in CC-

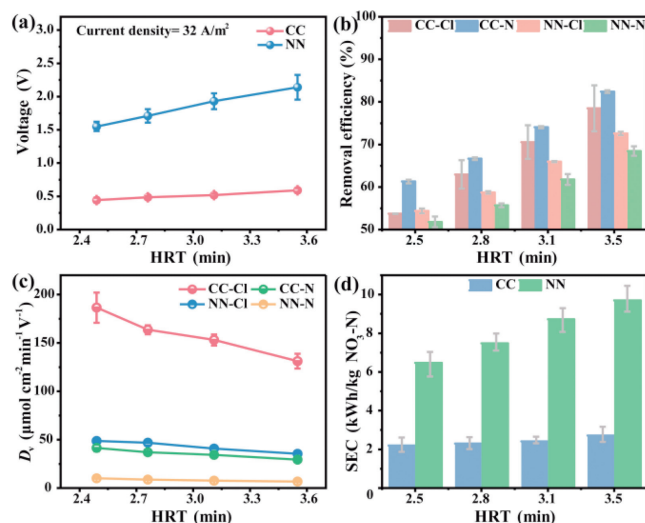


**Fig. 3.** Variations of (a) cell voltage, (b) NO<sub>3</sub>-N or Cl<sup>-</sup> removal efficiencies, (c)  $D_v$ , and (d) SEC as a function of the HRT. The experiments were carried out in a single-pass with the current density controlled at 32 A/m<sup>2</sup>. Each test was operated for a duration of 30 min.

FCDI (Fig. 3d). The efficiency of NO<sub>3</sub>-N removal in CC-FCDI was observed to increase and the SEC of NO<sub>3</sub>-N removal had a very small range of fluctuations as the HRT increased. The most favorable HRT duration has been established as 3.5 min.

Fig. 4a presents the LSV curve of CC-FCDI and NN-FCDI. Obviously, the current of CC-FCDI is significantly larger than that of NN-FCDI, a difference attributable primarily to the spacer types.

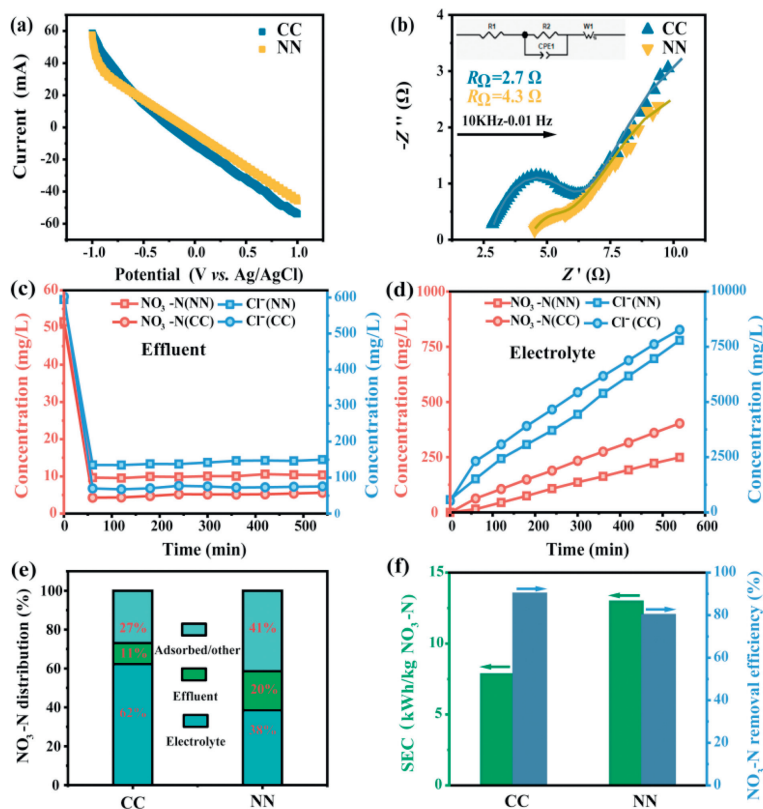


**Fig. 4.** (a) LSV scanning (-1.0~1.0 V vs. Ag/AgCl, 5 mV/s) of two devices. (b) Nyquist plots of FCDI cells with two spacers. The symbol  $Z'$  denotes the real component of impedance  $Z$ , while  $-Z''$  represents the imaginary component. The analysis of the EIS was carried out using NaCl concentrations of 1000 mg/L. The time course results of the following variables were analyzed: (c) the effluent concentration of NO<sub>3</sub>-N and Cl<sup>-</sup>, (d) the electrolyte concentration of NO<sub>3</sub>-N and Cl<sup>-</sup>, (e) the SEC and ion removal efficiency, and (f) the distributions of NO<sub>3</sub>-N in FCDI systems.

Fig. 4b illustrates the internal resistances of the FCDI systems, determined through EIS analysis [41]. The equivalent circuits of CC-FCDI and NN-FCDI were constructed based on previous studies [42]. The measured ohmic resistance of the CC-FCDI was determined to be 2.7  $\Omega$ , 37.2% lower than 4.3  $\Omega$  observed in NN-FCDI. In an FCDI system, spacer, membrane, feed water, and flow electrode all contributed to the internal ohmic resistance. Utilizing a non-conductive spacer, like NN, can elevate the FCDI's internal resistance, mainly due to the diminished volume of the electrolyte in the desalination compartment. Conversely, when incorporating a conductive spacer, such as CC, the FCDI exhibits a substantially reduced internal resistance. This reduction is attributed to the electric double layers formed on the surface of CC, which significantly accelerate the ion transfer in desalination chamber and mitigate the polarization near IEMs. A long-term experiment lasting 9 h was conducted to assess the efficiency of both systems for  $\text{NO}_3^-$ -N removal, employing optimal parameters of a current density of 32  $\text{A}/\text{m}^2$  and a HRT of 3.5 min. Over this extended operation, the voltage of both devices declined due to the ion accumulation within the electrodes (Fig. S6 in Supporting information), which resulted in a gradual counter-diffusion of ions from the electrode solution into the desalination chamber. The effluent conductivity of CC-FCDI and NN-FCDI were 288  $\mu\text{S}/\text{cm}$  and 505  $\mu\text{S}/\text{m}$  (Fig. S7 in Supporting information), respectively. As shown in Fig. 4c, the effluent of  $\text{NO}_3^-$  concentration remained stable, highlighting the stability of the system operation over an extended period. In Fig. 4d, the  $\text{NO}_3^-$ -N and  $\text{Cl}^-$  concentrations in CC-FCDI electrolyte was higher than those of NN-FCDI. Due to  $\text{Cl}^-$  accumulation in the electrolyte,  $\text{Cl}^-$  concentration gradient across the membrane increased, considerably inhibited  $\text{Cl}^-$  migration from the desalination chamber to the anode chamber. Similar behavior was observed for  $\text{NO}_3^-$ -N. Mass balance calculations revealed that 62.0% of  $\text{NO}_3^-$ -N in CC-FCDI was captured by electrodes, 11% remains in the effluent, while only 27.0% was found in the electrolyte (Fig. 4e). The concentrations of  $\text{NO}_3^-$ -N and  $\text{Cl}^-$  in the effluent from CC-FCDI were notably lower than in NN-FCDI, with  $\text{NO}_3^-$ -N levels in the electrolyte being neglected.

As shown in Fig. 4f, the SEC for  $\text{NO}_3^-$ -N removal increased considerably in the long-term operation compared to the single run. However, CC-FCDI still maintained a great advantage over NN-FCDI in terms of energy performance. Notably, CC-FCDI not only reduced the SEC but also improved the removal rate by about 10%. The  $\text{NO}_3^-/\text{Cl}^-$  selectivity during prolonged operation was enhanced due to the distinct transport gradients of the ions, influenced by the considerable concentration disparity between  $\text{NO}_3^-$ -N and  $\text{Cl}^-$  in the electrolyte. In summary, the results in this study offered a feasible approach to decrease the SEC for  $\text{NO}_3^-$ -N removal.

In this study, we thoroughly investigated of the influences of conductive spacer (*i.e.*, CC) and non-conductive spacer (*i.e.*, NN) on  $\text{NO}_3^-$ -N removal performances. At an HRT of 3.5 min and a current density of 32  $\text{A}/\text{m}^2$ , CC-FCDI achieved 82.4% nitrate removal at a current density of 32  $\text{A}/\text{m}^2$ , 15% higher than that of NN-FCDI. In addition, the SEC for nitrate removal in CC-FCDI was 72.0% lower than that of the control experiments with NN-FCDI. Electrochemical tests such as LSV and EIS revealed that the internal resistance of FCDI was significantly reduced when using CC as the spacer. CC facilitated ion across the desalination because of its higher ion conductivity, *i.e.*, lower ionic resistance of EDLs than the bulk electrolyte solution. Long-term operation showed that CC-FCDI still maintained 90% nitrate removal efficiency even after 9 h continuous operation. Our results demonstrated that conductive spacer can play an important role in FCDI system. Thus, in pursuit of process improvement, the incorporation of advanced materials science methodologies and dynamic simulation modeling techniques can

be leveraged to opt for spacer materials that are not only more economically viable but also characterized by enhanced durability and superior electrical conductivity.

### Declaration of competing interest

The authors declare that they have no known competing financial interests or personal relationships that could have appeared to influence the work reported in this paper.

### Acknowledgments

This research was supported by Shanxi Province Basic Research Program (Free Exploration Category) (No. 202203021221041), National Natural Science Foundation of China (No. 52300016), China Postdoctoral Science Foundation (No. 2023M733379) and Students Innovation and Entrepreneurship Foundation of USTC (No. CY2022G12).

### Supplementary materials

Supplementary material associated with this article can be found, in the online version, at doi:10.1016/j.ccl.2023.109325.

### References

- [1] C.L. Ford, Y.J. Park, E.M. Matson, et al., *Science* 354 (2016) 741–743.
- [2] T.M. Mubita, J.E. Dykstra, P.M. Biesheuvel, et al., *Water Res.* 164 (2019) 114885.
- [3] D.I. Kim, R.R. Gonzales, P. Dorji, et al., *Desalination* 484 (2020) 114425.
- [4] M.H. Ward, T.M. deKok, P. Levallois, et al., *Environ. Health Perspect.* 113 (2005) 1607–1614.
- [5] M. Shrimali, K.P. Singh, *Environ. Pollut.* 112 (2001) 351–359.
- [6] C. Fenech, L. Rock, K. Nolan, et al., *Water Res.* 46 (2012) 2023–2041.
- [7] L. Gan, Y. Wu, H. Song, et al., *Sep. Purif. Technol.* 212 (2019) 728–736.
- [8] O. Pastushok, F. Zhao, D.L. Ramasamy, et al., *Chem. Eng. J.* 375 (2019) 121943.
- [9] K. Velusamy, S. Periyasamy, P.S. Kumar, et al., *Environ. Chem. Lett.* 19 (2021) 3165–3180.
- [10] S. Duan, T. Tong, S. Zheng, et al., *Water Res.* 173 (2020) 115571.
- [11] X. Meng, D.A. Vaccari, J. Zhang, et al., *Environ. Sci. Technol.* 48 (2014) 1541–1548.
- [12] M. Aliaskari, A.I. Schäfer, *Water Res.* 190 (2021) 116683.
- [13] X. Zou, J. Xie, C. Wang, et al., *Chin. Chem. Lett.* 34 (2023) 107908.
- [14] T. Feng, F. Li, X. Hu, et al., *Chin. Chem. Lett.* 34 (2023) 107862.
- [15] K.H. Kim, H. Lee, X. Huang, et al., *Energy Environ. Sci.* 16 (2023) 663–672.
- [16] F. Ni, Y. Ma, J. Chen, et al., *Chin. Chem. Lett.* 32 (2021) 2073–2078.
- [17] S. Wang, B. Shao, J. Qiao, et al., *Front. Environ. Sci. Eng.* 15 (2021) 80.
- [18] K. Fang, F. Peng, H. Gong, et al., *Front. Environ. Sci. Eng.* 15 (2021) 8.
- [19] S.A. Hawks, M.R. Cerón, D.I. Oyarzun, et al., *Environ. Sci. Technol.* 53 (2019) 10863–10870.
- [20] C. Hu, J. Dong, T. Wang, et al., *Chem. Eng. J.* 335 (2018) 475–482.
- [21] J.J. Lado, R.E. Pérez-Roa, J.J. Wouters, et al., *Sep. Purif. Technol.* 183 (2017) 145–152.
- [22] S.W. Tsai, L. Hackl, A. Kumar, et al., *Desalination* 497 (2021) 114764.
- [23] S. Jeon, H. Park, J. Yeo, et al., *Energy Environ. Sci.* 6 (2013) 1471–1475.
- [24] C. Zhang, D. He, J. Ma, et al., *Water Res.* 128 (2018) 314–330.
- [25] M.E. Suss, S. Porada, X. Sun, et al., *Energy Environ. Sci.* 8 (2015) 2296–2319.
- [26] J. Song, J. Ma, C. Zhang, et al., *Front. Chem.* 7 (2019) 146.
- [27] C. Zhang, J. Ma, L. Wu, et al., *Environ. Sci. Technol.* 55 (2021) 4243–4267.
- [28] F. Yang, J. Ma, X. Zhang, et al., *Water Res.* 164 (2019) 114904.
- [29] X. Zhang, H. Zhou, Z. He, et al., *Water Res.* 220 (2022) 118642.
- [30] X. He, W. Chen, F. Sun, et al., *Environ. Sci. Technol.* 57 (2023) 8828–8838.
- [31] L. Xu, S. Peng, Y. Mao, et al., *Water Res.* 216 (2022) 118290.
- [32] S. Dahiya, B.K. Mishra, *Sep. Purif. Technol.* 240 (2020) 116660.
- [33] D.A. Vermaas, M. Saakes, K. Nijmeijer, *J. Membr. Sci.* 453 (2014) 312–319.
- [34] K. Tang, H. Zheng, P. Du, et al., *Environ. Sci. Technol.* 56 (2022) 8885–8896.
- [35] J. Veerman, M. Saakes, S.J. Metz, et al., *J. Membr. Sci.* 327 (2009) 136–144.
- [36] P. Długolecki, J. Dąbrowska, K. Nijmeijer, et al., *J. Membr. Sci.* 347 (2010) 101–107.
- [37] K. Tang, K. Zhou, *Environ. Sci. Technol.* 54 (2020) 5853–5863.
- [38] L. Luo, Q. He, Z. Ma, et al., *Water Res.* 203 (2021) 117522.
- [39] L. Luo, Q. He, J. Ma, et al., *Desalination* 548 (2023) 116294.
- [40] R. Chen, X. Deng, C. Wang, et al., *Chem. Eng. J.* 435 (2022) 134845.
- [41] Z. Zhang, P. Zhu, C. Li, et al., *Chin. Chem. Lett.* 32 (2021) 154–157.
- [42] L. Xu, Y. Mao, Y. Zong, et al., *Water Res.* 190 (2021) 116782.